Organic & Biomolecular Chemistry

RSC Publishing

PAPER

View Article Online
View Journal | View Issue

Cite this: *Org. Biomol. Chem.*, 2013, **11**, 6414

Structure–activity studies of 4-phenyl-substituted 2′-benzoylpyridine thiosemicarbazones with potent and selective anti-tumour activity†

Adeline Y. Lukmantara,*[a] Danuta S. Kalinowski,[b] Naresh Kumar*[a] and Des R. Richardson*[b]

Received 28th May 2013,
Accepted 25th July 2013

DOI: 10.1039/c3ob41109e

www.rsc.org/obc

2′-Benzoylpyridine thiosemicarbazones (BpT) are effective iron chelators and display potent anti-proliferative activity against tumour cells. In order to gain greater insight into the structure–activity relationships of the BpT chelators, ten new analogues containing phenyl substituents at the N4-position of the BpT structure were synthesised. Importantly, aromatic substitution at the latter position of the BpT scaffold has not been previously explored and these studies represent the first attempt to investigate their structure–activity relationships. These compounds demonstrated significantly enhanced anti-proliferative activity compared to the clinically used iron chelator, desferrioxamine (DFO). Furthermore, the compounds showed appreciable therapeutic indices against cancer cells over normal cells *in vitro*. Structure–activity analysis revealed that electron-donating substituents such as $–CH_3$ and $–OCH_3$ resulted in greater anti-proliferative activity than electron-withdrawing groups such as –Br and –Cl. These findings help to elucidate the effect of a variety of 4-phenyl substituents on the biological activity of BpT series of chelators and facilitate the future development of thiosemicarbazones with improved anti-tumour activity.

Introduction

Thiosemicarbazones are derived from Schiff base condensation of thiosemicarbazides (*e.g.*, $H_2N–HN–CS–NH_2$) with aldehydes and ketones.[1] Due to their rich biological activity, thiosemicarbazones have attracted significant attention from the pharmaceutical industry over the last 50 years.[1] This focus has been primarily due to their anti-viral,[2,3] anti-bacterial[4–6] and anti-cancer activities.[7,8] Thiosemicarbazones are well-known as complexing agents, as they are able to chelate transition metals such as iron, copper and zinc to form metal complexes with potential biological activity.[9]

The conjugated N–N–S tridentate ligand system in thiosemicarbazones is particularly important for anti-cancer activity.[10] Indeed, the N and S atoms act as "soft" electron donors that complex transition metals.[5,10,11] As an important aspect of their mode of action, the iron and copper complexes are then able to catalyse the formation of reactive oxygen species (ROS) such as the hydroxyl radical that can cause damage to DNA.[12–14]

Iron is an essential element as it is involved in numerous cellular processes such as energy production, oxygen transport, regulation of gene expression and DNA synthesis.[15–17] While normal and cancer cells typically share similar biochemical processes,[18–20] the increased requirement for iron in rapidly proliferating cells offers an avenue for marked and selective chemotherapeutic activity.[1,21] The higher demand for iron in tumour cells has been associated with enhanced expression of transferrin receptor 1 (TfR1), which is responsible for the uptake of iron from the iron transport protein, transferrin (Tf).[1,15] The increased iron requirement is in part due to the enhanced need of ribonucleotide reductase (RR).[1,15] Significantly, RR catalyses the rate-limiting step in the formation of deoxyribonucleotides from ribonucleotide precursors using a mechanism that directly involves iron in its active site.[22] Therefore, the inactivation of RR *via* iron deprivation would be expected to block DNA synthesis in tumour cells, thereby hindering their growth.[23] This hypothesis has spurred the development of numerous iron-chelating compounds as potential chemotherapeutic agents.[13,24,25]

Thiosemicarbazone-based chelators such as 2′-benzoylpyridine thiosemicarbazone (BpT) **1**, 2′-(3-nitrobenzoyl)pyridine thiosemicarbazone (NBpT) **2** and halogenated 2′-benzoylpyridine

[a]*School of Chemistry, University of New South Wales, Sydney, NSW 2052, Australia. E-mail: n.kumar@unsw.edu.au; Fax: +61-2-93856141; Tel: +61-2-9385 4698*
[b]*Molecular Pharmacology and Pathology Program, Department of Pathology and Bosch Institute, University of Sydney, Sydney, NSW 2006, Australia. E-mail: d.richardson@med.usyd.edu.au; Fax: +61-2-9036-6549; Tel: +61-2-9036-6548*

†CCDC 895056 and 895057. For crystallographic data in CIF or other electronic format see DOI: 10.1039/c3ob41109e

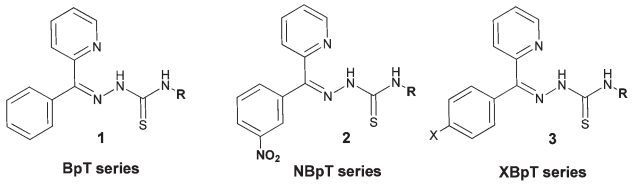

Fig. 1 Line drawings of the general structures of the BpT, NBpT and XBpT series of thiosemicarbazone chelators.

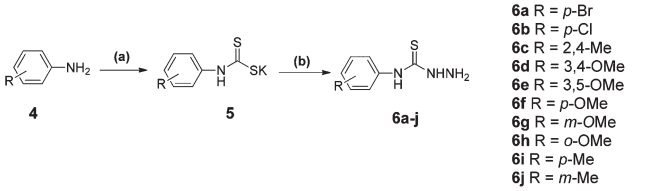

Scheme 1 Synthesis of 4-substituted phenyl thiosemicarbazides. Conditions and reagents: (a) CS_2, KOH, (b) $NH_2NH_2{\cdot}H_2O$.

thiosemicarbazones (XBpT) **3** have shown selective anti-tumour activity *in vitro* and *in vivo* (Fig. 1).[24,26] In particular, 2′-benzoylpyridine-4,4-dimethyl-3-thiosemicarbazone (Bp44mT) showed potent anti-tumour activity in nude mice bearing human DMS-53 lung cancer xenografts without causing cardiac toxicity or appreciable weight loss, even when administered orally at relatively high doses.[27] Recently, the halogenated XBpT series of ligands were shown to exhibit significant therapeutic indices for neoplastic over normal cells and improved anti-proliferative activity compared to the parent BpT compounds.[26]

It has been suggested that part of the anti-tumour activity of thiosemicarbazones involves the oxidation of chelated iron(II) to iron(III), releasing an electron to the tyrosyl free radical of RR to inactivate the enzyme.[28,29] The iron(III) complex can then be reduced by cellular thiols such as glutathione.[28] The facile inter-conversion of thiosemicarbazone iron complexes between the iron(II) and iron(III) states makes them ideal catalysts for Fenton chemistry.[13,24,26] Indeed, the ability of these complexes to redox cycle and generate reactive oxygen species (ROS) has been shown to correlate with their anti-tumour activity.[12,13,24] Moreover, the $Fe^{II/III}$ redox potentials of the thiosemicarbazone complexes can be fine-tuned by the incorporation of electron-donating or electron-withdrawing substituents on the thiosemicarbazone scaffold.[24,30]

In the present study, we have examined the effect of structural modifications on the complexation and biological activity of thiosemicarbazone chelators. We herein report the synthesis and molecular characterisation of a series of novel 4-phenyl substituted BpT ligands. To assess structure–activity relationships, we have examined their anti-proliferative activity, redox effects and ability to induce iron mobilisation from cells and inhibit iron uptake from transferrin. This investigation represents the first attempt to incorporate substitutions at the N4-position of the pendant phenyl group in the BpT scaffold.

Results and discussion

Chemistry

Substituted phenyl thiosemicarbazides were synthesised by the reaction of CS_2 with substituted anilines **4** in the presence of KOH in EtOH.[31] Initially, a "one-pot" reaction was attempted whereby the dithiocarbamate salt intermediate was directly reacted with an equimolar amount of $NH_2NH_2{\cdot}H_2O$. However, the desired product was not obtained. Therefore, the synthesis was conducted over two steps starting with the reaction of excess CS_2 with substituted anilines **4** and KOH under reflux (Scheme 1). The intermediate potassium dithiocarbamate salt **5** was filtered off and then heated at reflux for 6 h with a 20-fold excess of $NH_2NH_2{\cdot}H_2O$. The crude product mixture was washed, extracted with CH_2Cl_2 and recrystallised from CH_2Cl_2–*n*-hexane to yield the desired substituted phenyl thiosemicarbazide products **6a–j**. The characteristic C=S carbon atom of the 4-substituted phenyl thiosemicarbazides appeared at approximately 179 ppm in their ^{13}C NMR spectra.

The 4-substituted phenyl thiosemicarbazides **6a–j** were then reacted with 2′-benzoylpyridine **7** (1 : 1 mol ratio) in the presence of HCl to afford the 2′-benzoylpyridine 4-substituted phenyl thiosemicarbazones (Bp4(R)pT) **8a–j** *via* Schiff base condensation (Scheme 2).[13,32] The ^1H NMR spectrum of compound **8e** was characteristic of the thiosemicarbazones **8a–j**. The two singlet peaks at δ 3.76 and 3.80 corresponded to the two $-OCH_3$ groups of **8e** while the *para*-methyl substituent of **8i** showed a single peak at δ 2.34. The aromatic protons of **8e** occurred as doublets or triplets at δ 6.34–9.01. In addition, the NH protons appeared as singlets at δ 9.02 and 11.60. The ^{13}C NMR spectrum of **8e** indicated the disappearance of the C=O group in **7** and the formation of the new C=N bond at δ 147.40. Quaternary carbon peaks were observed at δ 126.50, 138.10, 136.71 and 147.40 with the C=S carbon atom resonance at δ 176.10. Notably, a combination of elemental analysis (C, H, N), UV, IR and HRMS was also used to confirm the purity and identity of all the compounds.

Final confirmation of the structures of the products was established through X-ray crystallography. Examples include compounds **8a** and **8i** (Fig. 2) that were found to crystallise in the triclinic $P\bar{1}$ space group with very similar unit cell parameters (axes). However, there are small differences in the orientation of the 6-membered rings attached to atom C1. The chemical structures of **8a** and **8i** indicate weak intra-molecular H-bonding (Fig. 2). Furthermore, the two analogues show a

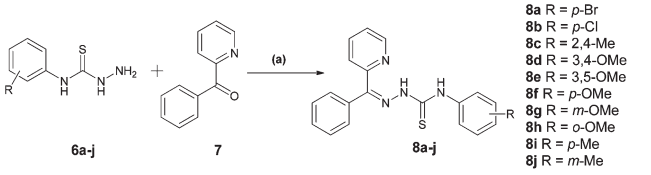

Scheme 2 Synthesis of 2′-benzoylpyridine 4-substituted phenyl thiosemicarbazones. Conditions and reagents: EtOH–HCl, reflux, 6 h, 95 °C.

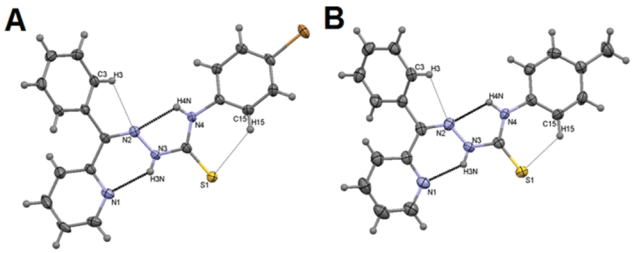

Fig. 2 ORTEP representation of **8a** and **8i** (thermal ellipsoids are drawn at 50% probability level).

very similar pattern of N–H···N, C–H···N and C–H···S bonding, which would be expected considering their structural similarities. The most significant interaction is N3–H3N···N1 in both the structures, which maintains the overall planarity of the molecule. The other rather weaker interactions, C13–H13···N2, N4–H4N···N2 and C15–H15···S1, are supportive in maintaining the planarity of the ligand.

Electrochemistry

Previous studies examining the BpT, NBpT and XBpT chelators have indicated that a correlation existed between anti-proliferative activity and their capability to undergo Fenton Chemistry upon complexation with intracellular iron.[13,24,26] Hence, it was important to investigate the electrochemical properties of the iron complexes formed from the novel thiosemicarbazone Bp4(R)pT derivatives **8a–j** as a key indicator of biological activity.

Cyclic voltammetry experiments revealed that compounds **8a–f** and **8h–j** exhibited totally reversible $Fe^{III/II}$ couples in MeCN–H_2O (7 : 3). This solvent combination was used to ensure sufficient solubility and to allow comparisons to previous studies using similar ligands and the same solvent mixture.[24,26] The redox potentials of the iron complexes of the novel thiosemicarbazones are shown in Table 1 in comparison to the iron complexes of their parent BpT compound, 2′-benzoylpyridine 4-phenyl-3-thiosemicarbazone ([Fe(Bp4pT)$_2$]).[24]

The redox potentials of **8c–f** and **8h–j**, which contain electron-donating substituents, were cathodically shifted by 9–63 mV relative to the iron complexes of Bp4pT (Table 1). On the other hand, the Fe complexes of **8a** and **8b**, which possess electron-withdrawing groups, demonstrated an anodic shift of 3–4 mV relative to Fe(Bp4pT)$_2$. These data are in good agreement with previous studies with the BpT group of chelators and other ligands which demonstrated that electron-withdrawing substituents increase redox potentials.[24,33–35] Generally, all the novel complexes tested showed redox values above +112 mV *versus* the normal hydrogen electrode (NHE). Unfortunately, the Fe complex of compound **8g** was not determined as the yield obtained was too low.

Table 1 $Fe^{III/II}$ redox potentials (MeCN–H_2O, 7 : 3) of the iron complexes of the Bp4(R)pT series

Ligand	R group	$Fe^{II/III}$ redox couple (mV *vs.* NHE)
[Fe(Bp4pT)$_2$]	H	+176
8a	Br	+179
8b	Cl	+180
8c	2,4-Me	+113
8d	3,4-OMe	+124
8e	3,5-OMe	+151
8f	*p*-OMe	+167
8g	*m*-OMe	ND
8h	*o*-OMe	+128
8i	*p*-Me	+140
8j	*m*-Me	+138

The experimental redox potential values suggest that the iron complexes of the Bp4(R)pT derivatives **8a–j** may be able to undergo redox cycling with intracellular oxidants and reductants to facilitate the generation of ROS. Thus, these compounds may exert their anti-proliferative effects *via* the generation of intracellular ROS. This possibility was examined further by assessing the oxidation of ascorbate (see below).

Biological studies

Anti-proliferative activity against tumour cells. The ability of thiosemicarbazones **8a–j** to inhibit cellular proliferation was assessed using human SK-N-MC neuroepithelioma cells. The effect of these novel ligands on the growth of SK-N-MC cells was examined as the effect of iron chelators on this cell type has been well characterised.[24] Furthermore, as positive controls we utilised the chelators desferrioxamine (DFO) and di-2-pyridylketone 4,4-dimethyl-3-thiosemicarbazone (Dp44mT), which show moderate and potent anti-tumour activities, respectively.[24,36] The anti-proliferative efficacy of both these agents has been well described by our laboratory using the SK-N-MC cell line.[24]

Previous studies have demonstrated that the BpT series of chelators have marked anti-proliferative activity *in vitro*[24] and *in vivo* against a human lung tumour xenograft in nude mice.[27] Since the novel 2′-benzoylpyridine 4-phenyl substituted thiosemicarbazone (Bp4(R)pT) derivatives (**8**) have a similar structure to BpT, it was anticipated that they would also show significant anti-cancer activity. In the present study, the Bp4(R)pT derivatives (**8**) were found to possess significantly ($p < 0.005$) greater anti-proliferative activity (IC_{50} = 0.016–0.115 μM) against SK-N-MC neuroepithelioma cells than the positive control chelator, DFO (IC_{50} = 21.73 ± 1.24 μM). As another control, we also examined the ligand, Dp44mT, which shows potent anti-proliferative activity against SK-N-MC cells.[24,37] However, the potency of the Bp4(R)pT was less than that of Dp44mT (IC_{50} = 0.002 ± 0.001 μM; Table 2). From all the novel ligands synthesised, 2′-benzoylpyridine 4-(*p*-methoxyphenyl)-3-thiosemicarbazone (Bp4(*p*-OMe)pT; **8f**) had the highest anti-proliferative activity with an IC_{50} value of 0.016 μM. The anti-tumour efficacy of **8a–j** was less potent than or similar to the parent BpT compound, namely 2′-benzoylpyridine 4-phenyl-3-thiosemicarbazone (Bp4pT, IC_{50} = 0.022 ± 0.003 μM).[24]

Initial structure–activity relationship (SAR) analysis suggested that thiosemicarbazones with electron-withdrawing substituents were less active than analogues bearing an electron-donating substituent. For example, the incorporation of Br **8a** or Cl **8b** substituents resulted in the lowest anti-proliferative activity of this series of ligands, with IC_{50} values of 0.115 ±

Table 2 IC_{50} μM values of Bp4(R)pT **8a–j** at inhibiting the growth of SK-N-MC neuroepithelioma cells and mortal MRC-5 lung fibroblasts as determined by the MTT assay. Results are means ± SD (3 experiments)

Ligand	SK-N-MC (μM)	MRC-5 (μM)	Log P_{calc}	Therapeutic index
DFO	21.73 ± 1.24			
Dp44mT	0.002 ± 0.001		2.19	
Bp4pT	0.022 ± 0.003	2.214 ± 0.25	4.43	100
8a	0.115 ± 0.028	2.170 ± 0.12	5.26	19
8b	0.082 ± 0.013	0.248 ± 0.11	4.99	3
8c	0.018 ± 0.002	0.216 ± 0.13	5.41	12
8d	0.032 ± 0.005	1.033 ± 1.59	4.18	32
8e	0.031 ± 0.003	1.811 ± 0.53	4.18	58
8f	0.016 ± 0.004	0.168 ± 0.18	4.31	10
8g	0.025 ± 0.004	2.723 ± 3.77	4.31	109
8h	0.044 ± 0.019	0.287 ± 0.64	4.31	7
8i	0.018 ± 0.006	1.372 ± 0.76	4.92	76
8j	0.041 ± 0.001	0.140 ± 0.18	4.92	3

0.028 and 0.082 ± 0.013 μM, respectively. In contrast, chelators **8c–j**, which bear electron-donating $-CH_3$ and $-OCH_3$ substituents, exhibited more potent anti-proliferative activity (IC_{50} = 0.016–0.044 μM). Interestingly, analogues bearing electron-donating substituents at the *para* position (*i.e.*, **8c**, **8f** and **8i**) demonstrated the most potent anti-proliferative effects (IC_{50} = 0.016–0.018 μM). These observations suggest that electron donors facilitate marked cytotoxic activity and this is an important factor for future ligand design.

The lipophilicity (log P_{calc}) of the chelators **8a–j** was also examined to determine whether it was correlated with anti-proliferative activity (Table 2). Generally, it was observed that chelators, **8a** and **8b**, with electron-withdrawing substituents (4-Br and 4-Cl) that have high log P_{calc} values of 5.26 and 4.99, respectively, possessed lower anti-proliferative activity compared to those compounds with electron-donating substituents that have log P_{calc} values of 4.18–4.92 (Table 2). However, from this initial analysis, it is not possible to judge whether the higher activity is due to lipophilicity or the electron-donating substituents. Considering this, the three chelators (**8c**, **8f** and **8i**) with the greatest anti-proliferative efficacy (0.016–0.018 μM) had log P_{calc} values which varied from 4.3 to 5.41 (Table 2). These values were similar to or exceeded that of the least effective analogues, **8a** and **8b**, with electron-donating substituents. This observation suggests that for this group of ligands, the electron-donating and -withdrawing properties of the substituents appear more important than lipophilicity in terms of anti-proliferative activity (Table 2). In fact, a previous study from our laboratory examining the BpT ligands demonstrated that aromatic substitution of the strongly electron-withdrawing *m*-nitro group on the phenyl ring located at the imine carbon (resulting in the NBpT series) increased the redox potential of the complexes which was detrimental to their redox activity and anti-proliferative efficacy.[24] Nonetheless, it is well known that optimal lipophilicity is an important criterion for the efficacy of chelators, including closely related ligands of the aroylhydrazone and thiosemicarbazone series.[38]

Anti-proliferative activity against normal cells. To determine the selectivity of the chelators **8a–j** towards tumour cells, their anti-proliferative activity against normal MRC-5 fibroblasts was also investigated (Table 2). The results showed that the compounds were significantly ($p < 0.05$) less cytotoxic against mortal cells compared to SK-N-MC tumour cells. *In vitro* therapeutic indices were calculated from the ratio of the IC_{50} values of MRC-5 cells *vs.* SK-N-MC cells (*i.e.*, IC_{50} (MRC-5)/IC_{50} (SK-N-MC)) with higher values representing greater selectivity. The therapeutic index values of the chelators in this study ranged from 3 to 109 (Table 2), with four of the analogues showing therapeutic index values of >50, indicating that the ligands were moderately to highly selective for tumour cells over normal cells. Compound **8g** was found to be the most selective of all the ligands examined, with a therapeutic index value of 109. Furthermore, the three most cytotoxic analogues in this series (*i.e.* **8c**, **8f** and especially **8i**) showed appreciable selectivity for tumour cells over normal cells with therapeutic index values of 10–76. The potent anti-proliferative activity and selectivity towards cancer cells of these analogues make them ideal candidates for further investigation of their anti-neoplastic properties.

Anti-proliferative activity of iron complexes against tumour cells. The effect of complexation on the anti-proliferative behaviour of the Bp4(R)pT chelators (**8a–j**) against SK-N-MC neuroepithelioma cells was also examined. The results showed that the anti-proliferative activities of the iron complexes were 3- to 300-fold less potent compared to the respective free ligands (Table 3). Significantly, all of the iron complexes showed IC_{50} values of >0.43 μM (Table 3), while their free ligands had IC_{50} values <0.12 μM (Table 2). This observation could possibly be attributed to the lack of ability of the pre-formed complexes to sequester intracellular iron from cellular enzymes such as ribonucleotide reductase that are responsible for facilitating cellular proliferation.[13] This is in agreement with earlier studies conducted using the BpT analogues, where a 2- to 200-fold decrease in anti-proliferative activity was observed for the iron complexes compared with the free ligands.[24] This suggests that the new derivatives (**8**) may have a similar mode of action to the original BpT compounds.[24]

Table 3 IC_{50} (μM) values of the iron complexes of the Bp4(R)pT chelators **8a–j** at inhibiting the growth of SK-N-MC neuroepithelioma cells. Results are means ± SD (3 experiments). ND = not determined

Ligand	$Fe^{III}(L)_2ClO_4$ complex IC_{50} (μM)
Bp4pT	0.72 ± 0.01
8a	>6.25
8b	>6.25
8c	5.73 ± 0.26
8d	0.43 ± 0.1
8e	2.46 ± 0.04
8f	0.76 ± 0.19
8g	ND
8h	ND
8i	2.20 ± 0.67
8j	3.52 ± 0.48

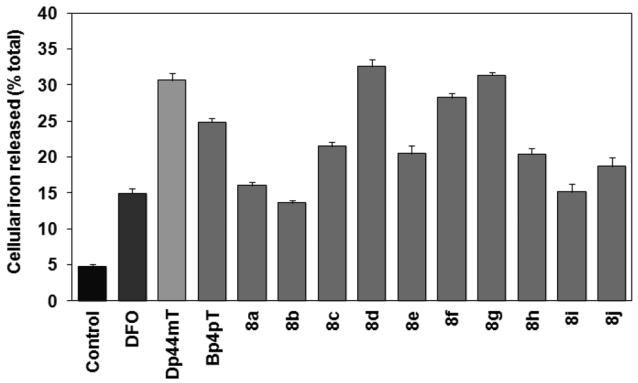

Fig. 3 Effect of the chelators **8a–j** on ^{59}Fe mobilisation from prelabelled SK-N-MC neuroepithelioma cells. Cells were labelled for 3 h at 37 °C with ^{59}Fe–Tf (0.75 μM) and washed 4 times at 4 °C with ice-cold PBS. The cells were then reincubated with a medium alone (control) or a medium containing the chelator (25 μM) for 3 h at 37 °C to assess cellular ^{59}Fe release. Results are means ± SDs of 3 experiments with 3 determinations in each experiment.

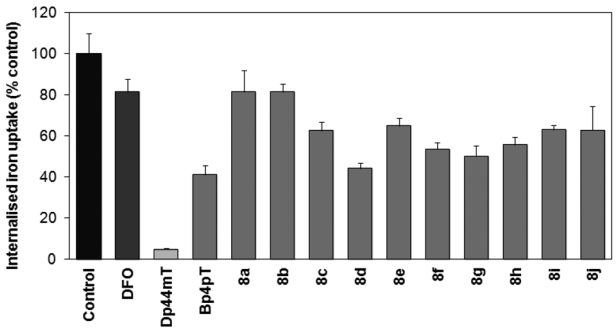

Fig. 4 Effect of the chelators **8a–j** on ^{59}Fe uptake from ^{59}Fe–transferrin by SK-N-MC neuroepithelioma cells. Cells were labelled for 3 h at 37 °C with ^{59}Fe–Tf (0.75 μM) in the presence of the chelator (25 μM) or its absence (control). The cells were then washed 4 times at 4 °C and incubated for 30 min at 4 °C with the protease, Pronase (1 mg mL^{-1}), to determine internalised ^{59}Fe uptake (see the Materials and methods section for details). Results are means ± SDs of 3 experiments with 3 determinations in each experiment.

Chelator-mediated ^{59}Fe efflux from cells. The ability of the Bp4(R)pT derivatives **8a–j** to mobilise intracellular ^{59}Fe from SK-N-MC neuroepithelioma cells prelabelled with ^{59}Fe–Tf was determined in order to evaluate the potential role of iron chelation efficacy in anti-proliferative activity (Fig. 3). The release of ^{59}Fe mediated by these ligands was compared to the positive controls DFO and Dp44mT, which have been characterised in detail using SK-N-MC cells (Fig. 3).[12,24,26]

DFO showed limited ^{59}Fe mobilisation efficacy, resulting in the release of only 15 ± 1% of intracellular ^{59}Fe, while the control (*i.e.*, culture medium alone) induced only 5 ± 1% of intracellular ^{59}Fe release (Fig. 3). The Bp4(R)pT chelators **8** exhibited moderate ^{59}Fe mobilisation activity, which resulted in a release of 16–33% of cellular ^{59}Fe. Compounds **8d** and **8g** showed the highest cellular ^{59}Fe release of 33% and 31% of cellular ^{59}Fe, respectively, being slightly more effective than the parent ligand, Bp4pT (Fig. 3). By comparison, the positive control Dp44mT mobilised 32 ± 1% of intracellular ^{59}Fe.

Incorporation of halogen substituents into chelators of this series (*i.e.*, ligands **8a** and **8b**) led to a significant ($p < 0.05$) decrease in ^{59}Fe mobilisation activity relative to the parent ligand, Bp4pT (Fig. 3). This may be related to several factors. First, the halogen substituents may withdraw electron density from the iron-binding site that could reduce iron chelation efficacy. Second, the increased lipophilicity due to halogenation may also lead to sequestration of the free ligand or iron complex in membranes, leading to lower iron chelation efficacy. The latter hypothesis is supported by the fact that three other ligands of this series that also showed log P_{calc} values >4.9 (namely **8c**, **8i** and **8j**) also showed lower ^{59}Fe mobilisation efficacy than the parent chelator, Bp4pT (Fig. 3).

It should be noted that the chelator-induced increase in cellular ^{59}Fe mobilisation was not mediated by their cytotoxic effects, as the cells remained >99% viable within the 3 h incubation used in these assays.

Chelator-mediated inhibition of cellular ^{59}Fe uptake from ^{59}Fe–Tf. For ligands to act as effective anti-proliferative agents, they must be able to mobilise intracellular iron, as well as prevent Fe uptake from the iron-binding protein, Tf.[38] Thus, the ability of the novel thiosemicarbazones (**8a–j**) to prevent ^{59}Fe uptake from ^{59}Fe–Tf was assessed using SK-N-MC neuroepithelioma cells, using DFO and Dp44mT as positive controls (Fig. 4).[12]

In agreement with previous studies,[24,39] DFO had little activity in preventing ^{59}Fe uptake from ^{59}Fe–Tf by cells, reducing it to only 82 ± 1% of the control, while Dp44mT decreased ^{59}Fe uptake to 5 ± 1% of the control. Relative to Dp44mT, all of the Bp4(R)pT ligands showed significantly ($p < 0.001$) less activity at preventing ^{59}Fe uptake from ^{59}Fe–Tf. In fact, the Bp4(R)pT series of chelators were either less effective or similarly effective as the parent ligand, Bp4pT (Fig. 4). Compounds **8d** and **8g** showed the greatest ability to prevent ^{59}Fe uptake among the novel chelators, inhibiting ^{59}Fe uptake to 41 ± 1% and 50 ± 1% of the control, respectively. Notably, **8d** and **8g** were also the most effective ligands at increasing ^{59}Fe mobilisation in the efflux assay (Fig. 3). Consistent with the results of the ^{59}Fe efflux assay, compounds **8a** and **8b** were the least effective and reduced ^{59}Fe uptake to only 81–82% of the control.

In order to further elucidate the role of optimum lipophilicity in enhancing the ability of the chelators to bind to cellular iron pools, the ^{59}Fe efflux or uptake activities of the compounds were plotted against their log P_{calc} values. The regression analysis showed a weak relationship between ^{59}Fe efflux or ^{59}Fe uptake relative to lipophilicity with R^2 values of 0.4384 and 0.4571, respectively (data not shown). Chelators with log P_{calc} values in the range of 4.18–4.31 (**8d** and **8g**) were the most effective at mobilising and inhibiting cellular ^{59}Fe, while highly lipophilic chelators (**8a**, **8b**, **8c**, **8i** and **8j**) (log P_{calc}: >4.9) showed lower Fe chelation efficacy.[24,40] This indicates the important role of optimal lipophilicity in facilitating the penetration of the chelators into the cell, thereby enhancing their ability to mobilise iron or inhibit iron uptake from Tf.

Ascorbate oxidation studies

The ability of iron complexes to undergo interconversion between the Fe(II) and Fe(III) states by interacting with cellular oxidants and reductants is an important factor in establishing a catalytic cycling mechanism to induce cytotoxicity. Thus, the ability of the iron complexes of the thiosemicarbazones **8a–j** to catalyse the oxidation of a physiologically relevant substrate, ascorbate, was evaluated. This assay assessed whether redox cycling may play a role in their anti-proliferative activity.

The iron complex of EDTA was used as a positive control in this investigation due to its ability to markedly increase ascorbate oxidation.[24,32,41] In all experiments, the results were expressed as iron-binding equivalents (IBEs) due to the different coordination modes of the ligands to iron. EDTA is hexadentate and forms 1 : 1 ligand–iron complexes, while compounds **8a–j** are tridentate, resulting in 2 : 1 ligand–iron complex formation. The IBE ratios of 0.1, 1 and 3 used in this study represent an excess of iron in comparison to the chelator, the complete filling of the coordination sphere or an excess of the chelator relative to iron, respectively.[13,41]

The iron complex of EDTA promoted high levels of ascorbate oxidation at IBEs of 1 and 3, while showing little activity at an IBE of 0.1 (Fig. 5). This is in agreement with previous studies illustrating the ability of the EDTA–iron complex to undergo facile redox cycling and catalyse ascorbate oxidation.[24,32]

In general, the iron complexes of compounds **8a–j** induced an increase in ascorbate oxidation to 136–270% and 143–321% at IBEs of 1 and 3, respectively, while showing little ascorbate oxidation at an IBE of 0.1 (Fig. 5). This result indicates that the chelators are able to bind to iron to form iron complexes that promote the oxidation of ascorbate *via* redox cycling. Among novel chelators **8a–j**, analogues **8d** and **8i** were the most effective at oxidising ascorbate (302% and 321% of the control, respectively, at an IBE of 3; Fig. 5). Interestingly, compound **8i** was also one of the most potent anti-proliferative ligands developed in this study. The compounds least effective at inducing ascorbate oxidation, particularly at an IBE of 3, were the halogenated ligands, **8a** and **8b** (Fig. 5). These results are in good agreement with these ligands having the highest redox potentials in this series (Table 1), making ascorbate oxidation more difficult. Similar results have been observed in our previous studies with other electron-withdrawing substituents on the thiosemicarbazone scaffold.[24] In general, the redox potentials of the iron complexes of **8c–j**, in particular, lie in a range that is accessible to cellular oxidants and reductants, enabling ascorbate oxidation. This observation indicates that like their parent BpT chelators,[24] ligands **8c–j** may induce their anti-proliferative effects, at least in part, by redox cycling and oxidative damage.

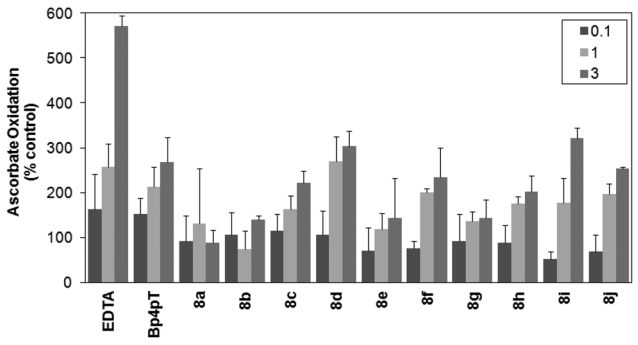

Fig. 5 Effect of the Fe^{III} complexes of **8a–j** on ascorbate oxidation. Chelators at iron-binding equivalent (IBE) ratios of 0.1, 1 and 3 were incubated in the presence of Fe^{III} (10 μM) and ascorbate (100 μM). The UV-vis absorbance at 265 nm was recorded after 10 and 40 min and the decrease of intensity between these time points was calculated.

Conclusions

The current investigation has revealed novel structure–activity relationships regarding aromatic substitution at the N4-phenyl moiety of 2′-benzoylpyridine thiosemicarbazones for the design of potent chelators for the treatment of cancer. The novel analogues **8a–j** exhibited markedly improved anti-proliferative activity to the well known chelator, DFO, while showing a similar potency to previously characterised BpT series of ligands.[24] Analogue **8f** was the most potent of the new series of ligands with an IC_{50} value of 0.016 μM. In addition, all of the novel thiosemicarbazones showed a similar or greater iron chelation efficacy than that of DFO, with ligand **8d** exhibiting the highest chelation efficacy overall. Hence, a direct correlation between anti-proliferative activity and iron chelation efficacy does not exist, with other factors such as redox activity *etc.* being important in terms of their cytotoxic effect.

Structure–activity analysis revealed that the ligands with electron-donating substituents generally possessed more potent anti-proliferative activity with Bp4(2,4-Me)pT (**8c**), Bp4(*p*-OMe)pT (**8f**), and Bp4(*p*-Me)pT (**8i**) having the lowest IC_{50} values of 0.018, 0.016 and 0.018 μM, respectively. On the other hand, those ligands containing electron-withdrawing substituents such as Bp4(*p*-Br)pT (**8a**) and Bp4(*p*-Cl)pT (**8b**) had markedly higher IC_{50} values of 0.082 and 0.155 μM, respectively. The halogenated chelators also showed reduced ability to mobilise intracellular iron and prevent ^{59}Fe uptake from Tf. Furthermore, the electron-withdrawing effects of the halogen substituents led to higher redox potentials and reduced ability to oxidise ascorbate. This reduction of redox activity may be responsible for their decreased anti-proliferative efficacy. Collectively, these observations strongly indicate that electron-withdrawing substituents should be avoided in terms of the design of BpT analogues in order to optimise their activity.

Notably, the analogue Bp4(3,4-OMe)pT (**8d**) was the most effective in mobilising intracellular ^{59}Fe as well as inhibiting ^{59}Fe uptake. In terms of selectivity, the novel thiosemicarbazones **8a–j** demonstrated appreciable therapeutic indices *in vitro*, indicating greater cytotoxicity for neoplastic cells relative to normal cells with the most selective analogues **8g** and **8i** exhibiting therapeutic index values of >75. In addition, the analogues **8d** and **8i** were also the most effective at oxidising ascorbate, suggesting that redox activity may play a significant

role in determining their anti-proliferative effects. Considering all the analogues in this series, ligand Bp4(*p*-Me)pT (**8i**) possessed the best overall combination of anti-proliferative activity, selectivity, and redox activity, and thus, represents a promising candidate for further *in vivo* evaluation.

In summary, a series of novel 2′-benzoylpyridine 4-phenyl substituted thiosemicarbazones **8a–j** that were synthesised have shown superior anti-proliferative and iron chelation efficacies compared to the well known chelator, DFO. Structure–activity relationship analysis indicated that the biological activities of these thiosemicarbazones were markedly influenced by the nature of the substituents that are placed on the pendant phenyl ring. The results of this study are anticipated to contribute to the further design and development of more efficacious BpT chelators in the future.

Experimental section

General information

^{1}H and ^{13}C NMR spectra were obtained in the selected solvent on a Bruker DPX 300 spectrometer at the designated frequency and were internally referenced to the solvent peaks. Chemical shifts (δ) are in parts per million (ppm) downfield from TMS (δ); multiplicity; observed coupling constant (J) in hertz (Hz); proton count; assignment. Multiplicities are recorded as singlet (s), doublet (d), doublet of doublet (dd), doublet of triplet (dt), triplet (t), quarter (q), multiplet (m) and broad singlet (bs) where appropriate. Melting points were measured using a Mel-Temp melting point apparatus and are uncorrected. Microanalysis was performed using a Carlo Erba Elemental Analyzer EA 1108 at the Campbell Microanalytical Laboratory, University of Otago, New Zealand. Infrared Spectra were recorded using a Thermo Nicolet 370 FTIR spectrometer as KBr disks. Ultraviolet visible spectra were recorded using a Varian Cary 100 Scan Spectrometer in the designated solvents and data are reported as wavelength (λ) in nm and adsorption coefficient (ε) in cm^{-1} M^{-1}.

Gravity column chromatography was carried out using Grace Davison LC60A 40–63 micron silica gel. Flash chromatography was performed using Grace Davison LC60A 6–35 micron silica gel. Reactions were monitored using thin layer chromatography, performed using Merck DC aluminium plates coated with silica gel GF_{254}. Compounds were detected by short and long wavelength ultraviolet light.

All commercially available reagents were purchased from Fluka, Sigma Aldrich, Alfa Aesar and Lancester, and used without further purification. Desferrioxamine (DFO) was purchased from Novartis, Basel, Switzerland. All reactions requiring anhydrous conditions were performed under an argon/nitrogen atmosphere. Anhydrous solvents were obtained using a PureSolv MD Solvent Purification System.

General procedure for the synthesis of 6a–j

CS_2 (8 mL) was added to a mixture of the respective aniline (5 g, 0.04 mol) and KOH (5 g, 0.09 mol) in 100 mL of ethanol. The reaction was stirred at room temperature for 2 h. An additional 3 mL of CS_2 was added and the mixture was heated to reflux for 2 h. The reaction was cooled, poured into water (100 mL) and stirred at room temperature overnight. The precipitate was filtered to obtain the intermediate potassium phenylcarbamodithioate. This intermediate was further reacted with $NH_2NH_2{\cdot}H_2O$ (20 mol) in 100 mL of ethanol and the mixture was heated at reflux for 6 h. The resulting mixture was extracted with CH_2Cl_2 and washed with sat. NaCl. The organic layer was dried over anhydrous Na_2SO_4 and reduced under pressure. The residue was recrystallised from CH_2Cl_2–*n*-hexane.

***p*-Bromophenyl thiosemicarbazide (6a).** Grey solid (1.238 g, 48%); mp 193–195 °C, lit.[42] 189 °C; ^{1}H NMR (300 MHz, DMSO-d_6) δ 4.87 (bs, 2H, NH_2), 7.44 (d, J = 8.93 Hz, 2H, ArH), 7.63 (d, J = 7.94 Hz, 2H, ArH), 9.21 (s, 1H, NH), 9.34 (s, 1H, NH).

***p*-Chlorophenyl thiosemicarbazide (6b).** White greyish powder (1.242 g, 43%); mp 196–198 °C, lit.[43] 190 °C; ^{1}H NMR (300 MHz, DMSO-d_6) δ 4.85 (bs, 2H, NH_2), 7.32 (d, J = 8.91 Hz, 2H, ArH), 7.68 (d, J = 7.66 Hz, 2H, ArH), 9.20 (s, 1H, NH), 9.27 (s, 1H, NH).

2,4-Dimethylphenyl thiosemicarbazide (6c). Yellow crystals (1.051 g, 40%); mp 145–148 °C, lit.[44] 150–152 °C; ^{1}H NMR (300 MHz, DMSO-d_6) δ 2.13 (s, 3H, CH_3), 2.24 (s, 3H, CH_3), 3.72 (s, 2H, NH_2), 6.96 (d, J = 8.19 Hz, 1H, ArH), 6.99 (s, 1H, ArH), 7.32 (d, J = 7.53 Hz, 1H, ArH), 8.99 (s, 1H, NH), 9.26 (s, 1H, NH).

3,4-Dimethoxyphenyl thiosemicarbazide (6d). Dark brown solid (1.068 g, 38%); mp 194–196 °C; λ_{max}(MeOH)/nm 222 (ε/M^{-1} cm^{-1} 36 819) and 243 (36 184); IR (KBr) ν_{max}/cm^{-1}: 3452, 3270, 3183, 2963, 2838, 2029, 1824, 1731, 1632, 1592, 1510, 1415, 1325, 1228, 1161, 1131, 1077, 1022, 981, 943, 912, 867, 833, 803, 765, 729, 711, 644, 598, 561, 516, 478, 438; ^{1}H NMR (300 MHz, DMSO-d_6) δ 3.70 (s, 3H, OCH_3), 3.71 (s, 3H, OCH_3), 4.73 (bs, 2H, NH_2), 6.85 (d, J = 8.65 Hz, 1H, ArH), 7.08 (s, 1H, ArH), 7.33 (s, 1H, ArH), 8.99 (s, 1H, NH), 9.51 (s, 1H, NH); ^{13}C NMR (75.6 MHz, DMSO-d_6) δ 55.83 (OCH_3), 56.07 (OCH_3), 109.15 (C2), 111.71 (C5), 115.92 (C6), 132.90 (C1), 145.98 (*C*–OCH_3), 148.36 (*C*–OCH_3), 179.77 (C═S) δ 55.83 (OCH_3), 56.07 (OCH_3), 109.15 (C2), 111.71 (C5), 115.92 (C6), 132.90 (C1), 145.98 (*C*–OCH_3), 148.36 (*C*–OCH_3), 179.77 (C═S). HRMS (+ESI): Found m/z 228.0800, $[M + H]^+$ $C_9H_{14}N_3O_2S$ required 228.0801.

3,5-Dimethoxyphenyl thiosemicarbazide (6e). Brown solid (699 mg, 27%); mp 166–169 °C; λ_{max}(MeOH)/nm 219 (ε/M^{-1} cm^{-1} 44 138), 244 (47 808), and 263 (46 342); IR (KBr) ν_{max}/cm^{-1}: 3279, 3189, 3018, 2966, 2840, 1635, 1593, 1530, 1492, 1461, 1428, 1351, 1302, 1264, 1204, 1153, 1075, 1053 942, 920, 842, 834, 808, 707, 604, 579, 538, 493; ^{1}H NMR (300 MHz, $CDCl_3$) δ 3.71 (s, 6H, 2 × OCH_3), 6.29 (d, J = 4.4 Hz, 1H, ArH), 6.50 (d, J = 2.3 Hz, 2H, H2, H6), 6.78 (bs, 2H, NH_2), 7.19 (s, 1H, NH), 7.78 (s, 1H, NH); ^{13}C NMR (75.6 MHz, $CDCl_3$) δ 55.97 (2 × OCH_3), 99.35 (ArCH), 103.42 (2 × ArCH), 139.03 (ArC), 161.80 (2 × *C*–OCH_3), 179.61 (C═S). HRMS (+ESI): found m/z 228.0803, $[M + H]^+$ $C_9H_{14}N_3O_2S$ required 228.0801.

***p*-Methoxyphenyl thiosemicarbazide (6f).** Charcoal powder (1.103 g, 52%); mp 160–163 °C, lit.[45] 154–156 °C; ^{1}H NMR (300 MHz, DMSO-d_6) δ 3.71 (s, 3H, OCH_3), 4.70 (bs, 2H, NH_2),

6.85 (d, J = 9.01 Hz, 2H, ArH), 7.42 (d, J = 8.12 Hz, 2H, ArH), 8.96 (s, 1H, NH), 9.43 (s, 1H, NH).

***m*-Methoxyphenyl thiosemicarbazide (6g).** Yellow solid (464 mg, 28%); mp 162–165 °C, lit.[46] 161 °C; ^{1}H NMR (300 MHz, DMSO-d_6) 3.71 (s, 3H, OCH_3), 4.78 (bs, 2H, NH_2), 6.65 (dd, J = 6.0, 3.0 Hz, 1H, ArH), 7.17 (d, J = 6.7 Hz, 2H, ArH), 7.47 (s, 1H, ArH), 9.13 (s, 1H, NH), 10.21 (s, 1H, NH).

***o*-Methoxyphenyl thiosemicarbazide (6h).** Brown solid (964 mg, 46%); mp 160–164 °C, lit.[47] 158–159 °C; ^{1}H NMR (300 MHz, DMSO-d_6) 3.82 (s, 3H, OCH_3), 4.83 (bs, 2H, NH_2), 6.87 (dd, J = 6.0, 3.0 Hz, 1H, ArH), 7.01-7.04 (m, 2H, ArH), 8.72 (d, J = 7.9 Hz, 1H, ArH), 9.18 (s, 1H, NH), 9.93 (s, 1H, NH).

***p*-Methylphenyl thiosemicarbazide (6i).** Pink powder (596 mg, 30%); mp 142–144 °C, lit.[48] 140–142 °C; ^{1}H NMR (300 MHz, DMSO-d_6) δ 2.25 (s, 3H, CH_3), 4.74 (bs, 2H, NH_2), 7.07 (d, J = 8.4 Hz, 2H, ArH), 7.47 (d, J = 8.8 Hz, 2H, ArH), 9.03 (s, 1H, NH), 9.61 (s, 1H, NH).

***m*-Methylphenyl thiosemicarbazide (6j).** Light pink powder (590 mg, 28%); mp 126–128 °C, lit.[49] 100–111 °C; ^{1}H NMR (300 MHz, DMSO-d_6) δ 2.26 (s, 3H, CH_3), 4.75 (bs, 2H, NH_2), 6.89 (d, J = 6 Hz, 1H, ArH), 7.15 (dd, J = 8.2, 6.1 Hz, 1H, ArH), 7.43 (d, J = 3 Hz, 2H, ArH), 9.06 (s, 1H, NH), 9.60 (s, 1H, NH).

General procedure for the synthesis of 8a–j

2′-Benzoylpyridine (7.3 mmol) was reacted with the appropriate substituted 4-phenyl thiosemicarbazide (7.3 mmol) in ethanol (25 mL). A few drops of concentrated HCl (32%) were added as a catalyst and the solution was heated to reflux for 6 h. The resulting mixture was concentrated by rotary evaporation. The precipitate formed upon cooling was collected by vacuum filtration and recrystallised from CH_2Cl_2–*n*-hexane.

2′-Benzoylpyridine 4-(*p*-bromophenyl)-3-thiosemicarbazone (8a). Light brown solid (233 mg, 53%); mp 179–182 °C; found: C, 55.2; H, 3.7; N, 13.7. Calc. for $C_{19}H_{15}BrN_4S$: C, 55.4; H, 3.7; N, 13.6%; λ_{max}(MeOH)/nm 203 (ε/M^{-1} cm^{-1} 8391) and 256 (4854); IR (KBr) ν_{max}/cm^{-1}: 3274, 3140, 3056, 1586, 1537, 1488, 1453, 1393, 1299, 1250, 1201, 1169, 1104, 1069, 1008, 927, 823, 789, 762, 742, 702, 660, 646, 622, 603, 531, 498, 455; ^{1}H NMR (300 MHz, $CDCl_3$) δ 7.34 (d, J = 8.0 Hz, 2H, ArH), 7.48–7.51 (m, 5H, ArH), 7.53–7.56 (m, 2H, ArH), 7.61–7.70 (m, 2H, ArH), 7.76 (d, J = 8.1 Hz, 2H, ArH), 9.49 (s, 1H, NH), 14.18 (s, 1H, NH); ^{13}C NMR (75.6 MHz, $CDCl_3$) δ 118.72 (*C*–Br), 124.40 (2 × ArCH), 125.52 (ArCH), 126.43 (ArCH), 128.55 (2 × ArCH), 129.13 (2 × ArCH), 129.36 (ArCH), 131.62 (2 × ArCH), 137.10 (ArC), 137.25 (ArCH), 137.30 (ArC), 142.93 (ArC), 148.54 (ArCH), 152.22 (C═N), 176.30 (C═S). HRMS (+ESI): found m/z 435.0060, $[M + Na]^+$; $C_{19}H_{15}{}^{79}BrN_4SNa$ required 435.0098.

2′-Benzoylpyridine 4-(*p*-chlorophenyl)-3-thiosemicarbazone (8b). Grey solid (216 mg, 37%); mp 175–177 °C; Found: C, 61.9; H, 4.0; N, 15.5. Calc. for $C_{19}H_{15}ClN_4S$: C, 62.2; H, 4.1; N, 15.3%; λ_{max}(MeOH)/nm 261 (ε/M^{-1} cm^{-1} 3235); IR (KBr) ν_{max}/cm^{-1}: 3274, 3134, 3053, 1589, 1534, 1493, 1458, 1397, 1310, 1251, 1200, 1168, 1104, 1077, 1031, 1012, 999, 927, 826, 793, 764, 742, 702, 646, 625, 607, 501, 467, 435; ^{1}H NMR (300 MHz, $CDCl_3$) δ 7.26–7.39 (m, 4H, ArH), 7.40–7.48 (m, 2H, ArH), 7.47–7.58 (m, 5H, ArH), 7.64–7.68 (m, 2H, ArH), 9.50 (s, 1H, NH), 14.18 (s, 1H, NH); ^{13}C NMR (75.6 MHz, $CDCl_3$) δ 124.42 (ArCH), 125.79 (2 × ArCH), 125.94 (ArCH), 126.44 (2 × ArCH), 128.56 (ArCH), 128.65 (ArCH), 129.14 (ArCH), 129.37 (2 × ArCH), 129.86 (ArC), 130.90 (C-Cl), 136.59 (ArC), 137.28 (ArCH), 142.97 (ArC), 148.51 (ArCH), 152.20 (C═N), 176.37 (C═S). HRMS (+ESI): found m/z 389.0591, $[M + Na]^+$ $C_{19}H_{15}{}^{35}ClN_4SNa$ required 389.0604.

2′-Benzoylpyridine 4-(2,4-dimethylphenyl)-3-thiosemicarbazone (8c). Light yellow crystals (299 mg, 60%); mp 105–110 °C; Found: C, 69.7; H, 5.8; N, 15.7. Calc. for $C_{21}H_{20}N_4S$: C, 69.9; H, 5.6; N, 15.5%; λ_{max}(MeOH)/nm 261 (ε/M^{-1} cm^{-1} 12 032), 308 (14 347) and 334 (18 384); IR (KBr) ν_{max}/cm^{-1}: 3314, 3093, 3051, 3015, 2838, 2561, 1608, 1541, 1474, 1352, 1336, 1309, 1261, 1239, 1206, 1155, 1075, 1001, 961, 940, 837, 779, 736, 707, 667, 580, 502; ^{1}H NMR (300 MHz, $CDCl_3$) δ 2.30 (s, 3H, CH_3), 2.33 (s, 3H, CH_3), 7.04–7.07 (m, 2H, ArH), 7.35–7.47 (m, 5H, ArH), 7.53–7.57 (m, 3H, ArH), 7.79 (d, J = 7.8 Hz, 1H, ArH), 8.85 (d, J = 6.8 Hz, 1H, ArH), 9.23 (s, 1H, NH), 13.95 (s, 1H, NH); ^{13}C NMR (75.6 MHz, $CDCl_3$) δ 17.91 (CH_3), 21.02 (CH_3), 124.27 (ArCH), 126.22 (ArCH), 126.97 (ArCH), 127.03 (ArCH), 128.49 (2 × ArCH), 129.05 (ArCH), 129.26 (2 × ArCH), 129.72 (ArCH), 131.25 (ArCH), 133.88 (2 × ArC), 137.20 (ArCH), 137.47 (*C*–CH_3), 142.68 (*C*–CH_3), 148.61 (ArC), 152.24 (C═N), 177.63 (C═S). HRMS (+ESI): found m/z 383.1288, $[M + Na]^+$ $C_{21}H_{20}N_4SNa$ required 383.1306.

2′-Benzoylpyridine 4-(3,4-dimethoxyphenyl)-3-thiosemicarbazone (8d). Light brown solid (190 mg, 39%); mp 177–180 °C; found: C, 55.8; H, 4.9; N, 12.3. Calc. for $C_{21}H_{20}N_4O_2S{\cdot}0.9CH_2Cl_2$: C, 56.1; H, 4.7; N, 12.0%; λ_{max}(MeOH)/nm 210 (ε/M^{-1} cm^{-1} 69 751) and 330 (50 999); IR (KBr) ν_{max}/cm^{-1}: 3282, 3151, 3056, 2979, 2915, 1597, 1585, 1544, 1493, 1469, 1454, 1418, 1375, 1315, 1299, 1272, 1250, 1232, 1201, 1175, 1151, 1119, 1105, 1074, 1031, 998, 943, 817, 796, 782, 744, 716, 704, 651, 637, 613, 556, 499, 483; ^{1}H NMR (300 MHz, $CDCl_3$) δ 3.85 (s, 3H, OCH_3), 3.87 (s, 3H, OCH_3), 6.84 (d, J = 7.8 Hz, 1H, ArH), 7.33–7.43 (m, 5H, ArH), 7.47 (s, 1H, ArH), 7.68–7.71 (m, 3H, ArH), 7.79 (d, J = 6 Hz, 1H, ArH), 8.19 (d, J = 9 Hz, 1H, ArH), 8.99 (s, 1H, NH), 11.57 (s, 1H, NH); ^{13}C NMR (75.6 MHz, $CDCl_3$) δ 55.88 (OCH_3), 55.97 (OCH_3), 109.99 (ArCH), 110.45 (ArCH), 117.88 (ArCH), 125.19 (ArCH), 125.61 (ArCH), 126.45 (ArC), 128.57 (2 × ArCH), 130.97 (2 × ArCH), 131.26 (ArC), 131.89 (ArCH), 136.62 (*C*–OCH_3), 143.09 (ArCH), 145.50 (ArCH), 147.20 (*C*–OCH_3), 147.44 (ArC), 148.34 (C═N), 175.77 (C═S). HRMS (+ESI): found m/z 393.1369, $[M + H]^+$ $C_{21}H_{21}N_4O_2S$ required 393.1385.

2′-Benzoylpyridine 4-(3,5-dimethoxyphenyl)-3-thiosemicarbazone (8e). Dark orange solid (215 mg, 45%); mp 198–202 °C; found: C, 58.9; H, 4.9; N, 13.3. Calc. for $C_{21}H_{20}N_4O_2S{\cdot}0.51CH_2Cl_2$: C, 59.3; H, 4.9; N, 12.9%; λ_{max}(MeOH)/nm 257 (ε/M^{-1} cm^{-1} 12 844) and 334 (11 239); IR (KBr) ν_{max}/cm^{-1}: 34470, 3169, 3087, 2955, 2936, 2833, 2576, 1603, 1567, 1533, 1513, 1469, 1451, 1408, 1352, 1336, 1306, 1263, 1235, 1210, 1179, 1137, 1103, 1024, 993, 849, 800, 775, 713, 730, 676, 582; ^{1}H NMR (300 MHz, $CDCl_3$) δ 3.80 (s, 6H, 2 × OCH_3), 6.34 (s, 1H, ArH), 7.22 (d, J = 2.2 Hz, 2H, ArH), 7.36–7.44 (m, 3H, ArH), 7.69–7.71 (m, 3H, ArH), 7.81 (d, J = 6 Hz,

1H, ArH), 8.23 (d, J = 7.5 Hz, 2H, ArH), 9.02 (s, 1H, NH), 11.56 (s, 1H, NH); ^{13}C NMR (75.6 MHz, $CDCl_3$) δ 55.45 (OCH_3), 99.36 (ArCH), 103.73 (2 × ArCH), 125.20 (ArCH), 125.68 (ArCH), 126.49 (ArC), 128.59 (2 × ArCH), 130.98 (2 × ArCH), 131.89 (ArCH), 136.75 (ArC), 139.68 (ArC), 143.08 (ArCH), 145.45 (ArCH), 147.46 (C═N), 160.18 (2 × C–OCH_3), 175.63 (C═S). HRMS (+ESI): Found m/z 393.1375, $[M + H]^+$ $C_{21}H_{21}N_4O_2S$ required 393.1385.

2′-Benzoylpyridine 4-(*p*-methoxyphenyl)-3-thiosemicarbazone (8f). Dark green needles (298 mg, 66%); mp 180–185 °C; found: C, 61.5; H, 5.0; N, 14.3. Calc. for $C_{20}H_{18}N_4OS{\cdot}1.5H_2O$: C, 61.7; H, 5.4; N, 14.4%; λ_{max}(MeOH)/nm 331 (ε/M^{-1} cm^{-1} 20 787); IR (KBr) ν_{max}/cm^{-1}: 3317, 3038, 2831, 2524, 1612, 1599, 1561, 1533, 1509, 1453, 1414, 1354, 1319, 1297, 1252, 1232, 1204, 1164, 1105, 1028, 979, 920, 836, 812, 772, 729, 711, 672, 622, 522, 509, 461; ^{1}H NMR (300 MHz, $CDCl_3$) δ 3.79 (s, 3H, OCH_3), 6.91 (d, J = 8.9 Hz, 2H, ArH), 7.32–7.56 (m, 5H, ArH), 7.66 (m, 3H, ArH), 7.77 (d, J = 8.1 Hz, 1H, ArH), 8.18 (d, J = 8.0, 2H, ArH), 8.98 (s, 1H, NH), 11.53 (s, 1H, NH); ^{13}C NMR (75.6 MHz, $CDCl_3$) δ 55.33 (OCH_3), 113.59 (ArCH), 124.28 (ArCH), 125.20 (ArCH), 126.38 (ArCH), 126.72 (ArC), 127.32 (2 × ArCH), 128.57 (2 × ArCH), 129.10 (ArCH), 130.86 (ArCH), 131.07 (ArC), 131.75 (ArCH), 137.19 (ArCH), 137.40 (ArC), 148.55 (ArCH), 152.27 (C═N), 157.81 (C–OCH_3), 176.29 (C═S). HRMS (+ESI): found m/z 363.1264, $[M + H]^+$ $C_{20}H_{19}N_4OS$ required 363.1280.

2′-Benzoylpyridine 4-(*m*-methoxyphenyl)-3-thiosemicarbazone (8g). Green powder (89 mg, 19%); mp 187–190 °C; found: C, 55.3; H, 4.5; N, 12.5. Calc. for $C_{20}H_{18}N_4OS{\cdot}1.1CH_2Cl_2$: C, 55.6; H, 4.5; N, 12.3%; λ_{max}(MeOH)/nm 257 (ε/M^{-1} cm^{-1} 21 307) and 334 (21 999); IR (KBr) ν_{max}/cm^{-1}: 3319, 3177, 3035, 2999, 2499, 1610, 1543, 1497, 1475, 1449, 1418, 1353, 1316, 1303, 1259, 1211, 1153, 1092, 1082, 1039, 989, 952, 867, 845, 775, 734, 703, 687, 578, 509; ^{1}H NMR (300 MHz, $CDCl_3$) δ 3.83 (s, 3H, OCH_3), 6.79 (s, 1H, ArH), 7.25 (d, J = 3.9 Hz, 2H, ArH), 7.37–7.40 (m, 3H, ArH), 7.47–7.53 (m, 2H, ArH), 7.69–7.70 (m, 3H, ArH), 7.81 (d, J = 6.5 Hz, 1H, ArH), 8.23 (d, J = 8.1 Hz, 1H, ArH), 8.99 (s, 1H, NH), 11.67 (s, 1H, NH); ^{13}C NMR (75.6 MHz, $CDCl_3$) δ 55.34 (OCH_3), 111.11 (ArCH), 112.80 (ArCH), 118.06 (ArCH), 125.18 (ArCH), 125.63 (ArCH), 126.47 (ArC), 128.58 (2 × ArCH), 128.87 (ArCH), 130.98 (ArCH), 131.89 (2 × ArCH), 136.65 (ArC), 139.16 (ArC), 143.09 (ArCH), 145.47 (ArCH), 147.48 (C═N), 159.39 (C–OCH_3), 175.93 (C═S). HRMS (+ESI): found m/z 363.1266, $[M + H]^+$ $C_{20}H_{19}N_4OS$ required 363.1280.

2′-Benzoylpyridine 4-(*o*-methoxyphenyl)-3-thiosemicarbazone (8h). Green powder (113 mg, 23%); mp 121–125 °C; found: C, 65.7; H, 5.0; N, 15.5. Calc. for $C_{20}H_{18}N_4OS{\cdot}0.1H_2O$: C, 65.9; H, 5.0; N, 15.4%; λ_{max}(MeOH)/nm 251 (ε/M^{-1} cm^{-1} 26 078) and 340 (29 385); IR (KBr) ν_{max}/cm^{-1}: 32417, 3048, 3007, 2968, 1600, 1583, 1545, 1466, 1443, 1419, 1333, 1299, 1249, 1227, 1179, 1150, 1113, 1074, 1044, 1029, 998, 936, 921, 798, 743, 699, 644, 507; ^{1}H NMR (300 MHz, $CDCl_3$) δ 3.83 (s, 3H, OCH_3), 6.84–6.95 (m, 3H, ArH), 7.02–7.26 (m, 2H, ArH), 7.34–7.41 (m, 2H, ArH), 7.54–7.57 (m, 3H, ArH), 7.76 (d, J = 7.7 Hz, 1H, ArH), 8.79–8.83 (m, 2H, ArH), 10.29 (s, 1H, NH), 13.58 (s, 1H, NH); ^{13}C NMR (75.6 MHz, $CDCl_3$) δ 55.77 (OCH_3), 110.18 (ArCH), 120.27 (ArCH), 121.26 (ArCH), 124.25 (ArCH), 124.80 (ArCH), 126.06 (ArCH), 127.69 (ArC), 128.32 (2 × ArCH), 128.97 (ArCH), 129.23 (2 × ArCH), 137.17 (ArCH), 137.46 (ArC), 142.30 (ArC), 148.65 (ArCH), 149.78 (C–OCH_3), 151.93 (C═N), 174.57 (C═S). HRMS (+ESI): found m/z 363.1267, $[M + H]^+$ $C_{20}H_{19}N_4OS$ required 363.1280.

2′-Benzoylpyridine 4-(*p*-methylphenyl)-3-thiosemicarbazone (8i). Pink powder (243 mg, 55%); mp 124–127 °C; found: C, 66.1; H, 5.1; N, 15.5. Calc. for $C_{20}H_{18}N_4S0.25CH_2Cl_2$: C, 66.1; H, 5.1; N, 15.2%; λ_{max}(MeOH)/nm 250 (ε/M^{-1} cm^{-1} 16 110) and 333 (17 553). IR (KBr) ν_{max}/cm^{-1}: 3287, 3054, 1595, 1546, 1534, 1467, 1442, 1418, 1319, 1303, 1271, 1250, 1202, 1171, 1106, 1075, 935, 922, 814, 796, 770, 702, 681, 666, 642, 612, 505, 471; ^{1}H NMR (300 MHz, $CDCl_3$) δ 2.35 (s, 3H, CH_3), 7.18 (d, J = 8.7 Hz, 2H, ArH), 7.33 (d, J = 8.0 Hz, 1H, ArH), 7.41 (d, J = 7.8 Hz, 1H, ArH), 7.45–7.48 (m, 3H, ArH), 7.51 (d, J = 8.1 Hz, 1H, ArH), 7.53–7.57 (m, 3H, ArH), 7.79 (d, J = 7.5 Hz, 1H, ArH), 8.86 (d, J = 5.4 Hz, 1H, ArH), 9.44 (s, 1H, NH), 14.01 (s, 1H, NH); ^{13}C NMR (75.6 MHz, $CDCl_3$) δ 21.00 (CH_3), 124.26 (ArCH), 124.43 (2 × ArCH), 126.26 (ArCH), 128.50 (2 × ArCH), 129.11 (2 × ArCH), 129.23 (2 × ArCH), 130.56 (ArCH), 135.36 (ArC), 135.75 (ArC), 137.17 (ArCH), 137.44 (C–CH_3), 142.58 (ArC), 148.57 (ArCH), 152.29 (C═N), 176.71 (C═S). HRMS (+ESI): found m/z 347.1319, $[M + H]^+$ $C_{20}H_{19}N_4S$ required 347.1330.

2′-Benzoylpyridine 4-(*m*-methylphenyl)-3-thiosemicarbazone (8j). White powder (163 mg, 36%); mp 190–193 °C; found: C, 61.5; H, 4.9; N, 14.3. Calc. for $C_{20}H_{18}N_4S{\cdot}0.65CH_2Cl_2$: C, 61.8; H, 4.8; N, 14.0%; λ_{max}(MeOH)/nm 331 (ε/M^{-1} cm^{-1} 19 295). IR (KBr) ν_{max}/cm^{-1}: 3482, 3443, 3321, 3184, 1612, 1549, 1522, 1495, 1481, 1448, 1340, 1316, 1225, 1211, 1164, 773; ^{1}H NMR (300 MHz, $CDCl_3$) δ 2.35 (s, 3H, CH_3), 7.03 (d, J = 7.5 Hz, 1H, ArH), 7.23 (s, 1H, ArH), 7.34–7.40 (m, 3H, ArH), 7.57 (dd, J = 7.2 Hz, 1H, ArH), 7.69–7.74 (m, 3H, ArH), 7.78 (d, J = 4.5 Hz, 2H, ArH), 8.19 (d, J = 7.5 Hz, 1H, ArH), 9.00 (d, J = 6 Hz, 1H, ArH), 9.48 (s, 1H, NH), 11.66 (s, 1H, NH); ^{13}C NMR (75.6 MHz, $CDCl_3$) δ 21.39 (CH_3), 123.27 (ArCH), 125.30 (ArCH), 125.60 (ArCH), 126.46 (ArC), 126.67 (ArCH), 127.29 (ArCH), 128.07 (2 × ArCH), 128.58 (ArCH), 130.95 (ArCH), 131.85 (2 × ArCH), 136.71 (ArC), 138.00 (ArC), 138.06 (C–CH_3), 143.06 (ArCH), 145.55 (ArCH), 147.35 (C═N), 176.26 (C═S). HRMS (+ESI): found m/z 347.1316, $[M + H]^+$ $C_{20}H_{19}N_4S$ required 347.1330.

2′-Benzoylpyridine 4-phenyl-3-thiosemicarbazone (Bp4pT). Orange solid (292 mg, 59%); mp 130–132 °C; found: C, 68.0; H, 4.8; N, 17.1. Calc for $C_{19}H_{16}N_4S{\cdot}0.15H_2O$: C, 68.1; H, 4.9; N, 16.7%; λ_{max}(MeOH)/nm 248 (ε/M^{-1} cm^{-1} 13 647) and 333 (17 093); IR (KBr) ν_{max}/cm^{-1}: 3299, 3050, 1594, 1533, 1498, 1469, 1439, 1417, 1367, 1318, 1303, 1271, 1253, 1204, 1173, 1107, 1074, 1047, 1029, 922, 798, 787, 756, 729, 704, 693, 673, 656, 644, 614, 606, 511, 498, 475; ^{1}H NMR (300 MHz, $CDCl_3$) δ 7.33–7.43 (m, 5H, ArH), 7.46–7.58 (m, 5H, ArH), 7.69 (m, 2H, ArH), 7.78 (m, 2H, ArH), 9.54 (s, 1H, NH), 14.06 (s, 1H, NH); ^{13}C NMR (75.6 MHz, $CDCl_3$) δ 124.11 (ArCH), 124.31 (ArCH), 124.59 (ArCH), 125.81 (ArCH), 126.32 (ArCH), 128.52 (ArCH), 128.63 (ArCH), 128.67 (ArCH), 129.12 (ArCH), 129.29 (ArCH), 129.82 (ArCH), 130.42 (ArCH), 137.21 (ArCH), 137.40 (ArC),

137.98 (ArC), 142.68 (ArC), 148.57 (ArCH), 152.26 (C=N), 176.44 (C=S). HRMS (+ESI): found *m/z* 355.0981, $[M + Na]^+$ $C_{19}H_{16}N_4SNa$ required 355.0993.

General procedure of the synthesis of $[Fe^{III}(Bp4(R)pT)_2]$ complexes

The desired Bp4(R)pT chelator (3.5 mmol) was dissolved in absolute EtOH (15 mL). A few drops of Et_3N were added to the solution followed by the addition of $Fe(ClO_4)_3{\cdot}6H_2O$ (1.7 mmol). The mixture was gently refluxed overnight. After cooling, the dark brown precipitate was filtered and washed with ethanol (5 mL).

$[Fe(Bp4(p\text{-}Br)pT)_2]H_2O$. Dark brown solid (117 mg, 11%); found: C, 50.9; H, 3.8; N, 12.4. Calc. for $C_{38}H_{28}Br_2FeN_8S_2{\cdot}H_2O$: C, 51.0.; H, 3.4; N, 12.5%. HRMS (+ESI): found *m/z* 875.5918, $[M]^+$; $C_{38}H_{28}{}^{79}Br_2{}^{56}FeN_8S_2$ required 875.9574.

$[Fe(Bp4(p\text{-}Cl)pT)_2]3.5H_2O$. Dark brown solid (46.4 mg, 43%); found: C, 53.9; H, 4.1; N, 12.9. Calc. for $C_{38}H_{28}Cl_2FeN_8S_2{\cdot}3.5H_2O$: C, 53.7; H, 4.2; N, 13.2%. HRMS (+ESI): found *m/z* 786.0594, $[M]^+$; $C_{38}H_{28}{}^{35}Cl_2{}^{56}FeN_8S_2$ required 786.0605.

$[Fe(Bp4(2,4\text{-}Me)pT)_2]ClO_4{\cdot}4H_2O$. Dark brown solid (15.5 mg, 14%); found: C, 53.4; H, 5.1; N, 11.4. Calc. for $C_{42}H_{38}ClFeN_8O_4S_2{\cdot}4H_2O$: C, 53.3; H, 4.9; N, 11.8%. HRMS (+ESI): found *m/z* 774.1990, $[M]^+$; $C_{42}H_{38}{}^{56}FeN_8S_2$ required 774.2010.

$[Fe(Bp4(3,4\text{-}OMe)pT)_2]ClO_4{\cdot}3H_2O$. Dark brown solid (30.5 mg, 29%); found: C, 50.7; H, 4.3; N, 10.9. Calc. for $C_{42}H_{38}ClFeN_8O_8S_2{\cdot}3H_2O$: C, 50.8; H, 4.5; N, 11.3%. HRMS (+ESI): found *m/z* 838.1631, $[M]^+$; $C_{42}H_{38}{}^{56}FeN_8O_4S_2$ required 838.1807.

$[Fe(Bp4(3,5\text{-}OMe)pT)_2]ClO_4{\cdot}8H_2O$. Dark brown solid (11.2 mg, 11%); found: C, 46.3; H, 4.9; N, 10.1. Calc. for $C_{42}H_{38}ClFeN_8O_8S_2{\cdot}8H_2O$: C, 46.6; H, 5.0; N, 10.4%. HRMS (+ESI): found *m/z* 838.1779, $[M]^+$; $C_{42}H_{38}{}^{56}FeN_8O_4S_2$ required 838.1807.

$[Fe(Bp4(p\text{-}OMe)pT)_2]ClO_4{\cdot}6.5H_2O$. Dark brown solid (57.5 mg, 54%); found: C, 48.3; H, 4.8; N, 11.2. Calc. for $C_{40}H_{34}ClFeN_8O_6S_2{\cdot}6.5H_2O$: C, 48.3; H, 4.8; N, 11.3%. HRMS (+ESI): found *m/z* 778.1576, $[M]^+$; $C_{40}H_{34}{}^{56}FeN_8O_2S_2$ required 778.1596.

$[Fe(Bp4(m\text{-}OMe)pT)_2]ClO_4{\cdot}3.75H_2O$. Dark brown solid (5.8 mg, 6%); found: C, 50.5; H, 4.1; N, 11.4. Calc. for $C_{40}H_{34}ClFeN_8O_6S_2{\cdot}3.75H_2O$: C, 50.8; H, 4.4; N, 11.8%. HRMS (+ESI): found *m/z* 778.1693, $[M]^+$; $C_{40}H_{34}{}^{56}FeN_8O_2S_2$ required 778.1596.

$[Fe(Bp4(p\text{-}Me)pT)_2]ClO_4$. Dark brown solid (31.5 mg, 28%); found: C, 56.5; H, 4.2; N, 13.0. Calc. for $C_{40}H_{34}ClFeN_8O_4S_2$: C, 56.8; H, 4.1; N, 13.2%. HRMS (+ESI): found *m/z* 746.1696, $[M]^+$; $C_{40}H_{34}{}^{56}FeN_8O_4S_2$ required 746.1697.

$[Fe(Bp4(m\text{-}Me)pT)_2]ClO_4{\cdot}H_2O$. Dark brown solid (7.5 mg, 7%); found C, 55.3; H, 4.4; N, 13.3. Calc. for $C_{40}H_{34}ClFeN_8O_4S_2{\cdot}H_2O$: C, 55.6; H, 4.2; N, 13.0%. HRMS (+ESI): found *m/z* 746.1687, $[M]^+$; $C_{40}H_{34}{}^{56}FeN_8O_4S_2$ required 746.1697.

Single crystal X-ray data for compounds 8a and 8i

Single crystals for X-ray diffraction of **8a** and **8i** were crystallised from ethanol or CH_2Cl_2–*n*-hexane. Suitable single crystals (for ligands **8a** and **8i**) were selected under a polarising microscope (Leica M165Z). These crystals were then loaded onto a MicroMount (MiTeGen, USA) consisting of a thin polymer tip with a wicking aperture. The X-ray diffraction measurements were carried out on a Bruker kappa-II CCD diffractometer at 150 K by using graphite-monochromated Mo-Kα radiation (λ = 0.710723 Å). The single crystals, mounted on the goniometer using cryo loops for intensity measurements, were coated with paraffin oil and then quickly transferred to the cold stream using an Oxford Cryo stream attachment. Symmetry related absorption corrections using the program SADABS[50] were applied and the data were corrected for Lorentz and polarisation effects using Bruker APEX2 software.[51] All structures were solved by direct methods and the full-matrix least-square refinements were carried out using SHELXL.[52] The non-hydrogen atoms were refined anisotropically. The molecular graphics was generated using Mercury.[53]

Crystal data of **8a**: molecular formula = $C_{19}H_{15}BrN_4S$. Formula weight = 411.32, crystal system = triclinic, space group = $P\bar{1}$, a = 9.5013 (5) Å, b = 10.0576 (5) Å, c = 10.2659 (5) Å, V = 858.00 (7) Å^3, T = 150 K, Z = 2, μ(Mo Kα) = 2.53 mm^{-1}, 12 449 reflection measured, 3011 independent reflections, 2609 observed reflections [$I > 2\sigma(I)$], R = 0.025. CCDC no. 895056.

Crystal data of **8i**: molecular formula = $C_{20}H_{18}N_4S$. Formula weight = 346.44, crystal system = triclinic, space group = $P\bar{1}$, a = 9.5261 (12) Å, b = 9.7850 (11) Å, c = 11.566 (2) Å, V = 874.4 (2) Å^3, T = 150 K, Z = 2, μ(Mo Kα) = 0.20 mm^{-1}, 11 680 reflection measured, 3070 independent reflections, 2098 observed reflections [$I > 2\sigma(I)$], R = 0.042. CCDC no. 895057.

Biological studies

Materials and methods

Cell culture. The human SK-N-MC neuroepithelioma and MRC-5 fibroblast cell lines were obtained from the American Type Culture Collection (ATCC, Manassas, VA, USA) and were grown at 37 °C in a humidified atmosphere of 5% CO_2/95% air in an incubator.[38] All cell lines were grown in Eagle's minimum essential medium (MEM; Invitrogen, Mulgrave, Victoria, Australia) supplemented with 10% (v/v) foetal calf serum (Commonwealth Serum Laboratories, Melbourne, Victoria, Australia), 1% (v/v) non-essential amino acids (Invitrogen), 1% (v/v) sodium pyruvate (Invitrogen), 2 mM L-glutamine (Invitrogen), 100 μg mL^{-1} of streptomycin (Invitrogen), 100 U mL^{-1} penicillin (Invitrogen), and 0.28 μg mL^{-1} of fungizone (Squibb Pharmaceuticals, Montreal, Canada).

Preparation of ^{59}Fe–transferrin. Human transferrin (Tf) (Sigma-Aldrich, St. Louis, MO, USA) was labeled with ^{59}Fe (Perkin-Elmer, Waltham, MA, USA) to produce $^{59}Fe_2$–Tf (^{59}Fe–Tf) by previously reported methods.[54,55]

The effect of chelators on cellular proliferation. The effect of the chelators on cellular proliferation was determined using the MTT [1-(4,5-dimethylthiazol-2-yl-)-2,5-diphenyl tetrazolium] assay.[24,38] The SK-N-MC cell line was seeded in 96-well microtitre plates at 1.5 × 10^4 cells per well in a medium

containing human ^{59}Fe–Tf (1.25 μM) and chelators or their iron complexes (0–25 μM). Chelators were dissolved in DMSO as 10 mM stock solutions and diluted in a medium containing 10% foetal calf serum (Commonwealth Serum Laboratories, Melbourne, Victoria, Australia) so that the final [DMSO] < 0.5% (v/v). At this final concentration, DMSO had no effect on proliferation.[38] Control samples contained a medium with human ^{56}Fe–Tf (1.25 μM) without the ligands or complexes. After a 72 h incubation, 10 μL of MTT (5 mg mL^{-1}) was added to each well and the cells were incubated for another 2 h at 37 °C. The cells were then lysed with 100 μL of 10% SDS–50% isobutanol in 10 mM HCl. The plates were then read at 570 nm using a scanning multiwall spectrophotometer. The inhibitory concentration (IC_{50}) was defined as the chelator concentration necessary to reduce the absorbance to 50% of the untreated control.

Effect of chelators on ^{59}Fe efflux from SK-N-MC cells. Iron efflux experiments examining the ability of various chelators to mobilise ^{59}Fe from SK-N-MC cells were performed using established techniques.[24,38,56] Briefly, following prelabelling of cells with ^{59}Fe–Tf (0.75 μM) for 3 h at 37 °C, the cell cultures were washed four times with ice-cold PBS. The cells were subsequently incubated with either control medium alone or the medium containing the chelator (25 μM) for 3 h at 37 °C. The overlying medium containing released ^{59}Fe was then separated from the cells using a Pasteur pipette. Radioactivity was measured in both the cell pellets and supernatant using a γ-scintillation counter (Wallace Wizard 3, Turku, Finland). In this study, the novel ligands were compared to the well characterised chelators DFO and Dp44mT.[12,38]

Effect of chelators on preventing ^{59}Fe uptake from ^{59}Fe–Tf by SK-N-MC cells. The ability of the chelators to prevent cellular ^{59}Fe uptake from ^{59}Fe–Tf in SK-N-MC cells was examined and performed using standard procedures.[12,24,38] Briefly, cells were incubated with ^{59}Fe–Tf (0.75 μM) for 3 h at 37 °C in the presence of a medium alone or in a medium containing each of the chelators (25 μM). The cells were then washed four times with ice-cold PBS and internalised ^{59}Fe was determined by placing the culture plates on ice and incubating the cell monolayer with the protease Pronase (1 mg mL^{-1}, Sigma) for 30 min at 4 °C. The cells were then removed from the monolayer using a plastic spatula and centrifuged at 12 000 rpm for 1 min. The supernatant represents membrane-bound, Pronase-sensitive ^{59}Fe, while the Pronase-insensitive fraction represents internalised ^{59}Fe.[24,54,55] In this assay, the novel chelators were compared to DFO and Dp44mT which are well characterised and acted as positive controls.[12,38] Radioactivity was assessed as described above.

Ascorbate oxidation assay. Ascorbic acid (100 μM) was prepared fresh prior to an experiment and incubated in the presence of Fe^{III} (10 μM; added as $FeCl_3$), a 50-fold molar excess of citrate (500 μM) and the chelator (1–60 μM). The chelators were dissolved in PBS buffer at high temperature. Absorbance at 265 nm was measured after 10 and 40 min at room temperature, and the decrease of intensity between these time points was calculated.[13,24,41,56]

Electrochemistry. Cyclic voltammetry was performed using a BAS100B/W potentiostat. A glassy carbon working electrode, an aqueous Ag/AgCl reference, and a Pt wire auxiliary electrode were used. All complexes were at *ca.* 1 mM concentration in MeCN–H_2O (7 : 3 v/v). This solvent combination was used to ensure solubility of all compounds. The supporting electrolyte was Et_4NClO_4 (0.1 M), and the solutions were purged with nitrogen prior to measurement. All potentials are cited *versus* the normal hydrogen electrode (NHE) by the addition of 196 mV to the potentials measured relative to the Ag/AgCl reference.

Statistical analysis. Experimental data were compared using a Student's *t*-test. Results were expressed as means ± SD (number of experiments).

Acknowledgements

This work was supported by a Project Grant from the National Health and Medical Research Council (NHMRC) Australia to D.R.R. [grant 632778] and D.S.K. [grant 1048972]; a NHMRC Senior Principal Research Fellowship to D.R.R. [grant 571123]; a Cancer Institute New South Wales Early Career Development Fellowship to D.S.K. [grant 08/ECF/1–30]; a Cancer Institute Research Innovation Grant to D.R.R. and D.S.K [grant 10/RFG/2–50]. The research was additionally supported by an ARC Discovery Grant (DP1095159) and a Linkage Project Grant (LP110200635). We thank Dr Mohan Bhadhade (Crystallography Laboratory, Analytical Centre, The University of New South Wales, Sydney, Australia) for collecting the X-ray crystal structure data.

Notes and references

1 D. S. Kalinowski and D. R. Richardson, *Pharmacol. Rev.*, 2005, **57**, 547.
2 A. Garoufis, S. K. Hadjikakou and N. Hadjiliadis, *Coord. Chem. Rev.*, 2009, **253**, 1384.
3 D. D. Perrin and H. Stünzi, *Pharmacol. Ther.*, 1981, **12**, 255.
4 M. Aslantas, E. Kendi, N. Demir, A. E. Sabik, M. Tümer and M. Kertmen, *Spectrochim. Acta, Part A*, 2009, **74**, 617.
5 A. A. Al-Amiery, A. A. H. Kadhum and A. B. Mohamad, *Bioinorg. Chem. Appl.*, 2012, 2012.
6 C. M. da Silva, D. L. da Silva, L. V. Modolo, R. B. Alves, M. A. de Resende, C. V. B. Martins and Â. de Fátima, *J. Adv. Res.*, 2011, **2**, 1.
7 W. X. Hu, W. Zhou, C. N. Xia and X. Wen, *Bioorg. Med. Chem. Lett.*, 2006, **16**, 2213.
8 I. Đilovic, M. Rubcic, V. Vrdoljak, S. K. Pavelic, M. Kralj, I. Piantanida and M. Cindric, *Bioorg. Med. Chem.*, 2008, **16**, 5189.
9 R. Setnescu, C. Barcutean, S. Jipa, T. Setnescu, M. Negoiu, I. Mihalcea, M. Dumitru and T. Zaharescu, *Polym. Degrad. Stab.*, 2004, **85**, 997.

10 D. S. Kalinowski and D. R. Richardson, *Chem. Res. Toxicol.*, 2007, **20**, 715.
11 G. Pelosi, *The Open Crystall. J.*, 2010, **3**, 16.
12 J. Yuan, D. B. Lovejoy and D. R. Richardson, *Blood*, 2004, **104**, 1450.
13 D. R. Richardson, P. C. Sharpe, D. B. Lovejoy, D. Senaratne, D. S. Kalinowski, M. Islam and P. V. Bernhardt, *J. Med. Chem.*, 2006, **49**, 6510.
14 D. B. Lovejoy, P. J. Jansson, U. T. Brunk, J. Wong, P. Ponka and D. R. Richardson, *Cancer Res.*, 2011, **71**, 5871.
15 D. R. Richardson, *Crit. Rev. Oncol. Hematol.*, 2002, **42**, 267.
16 M. W. Hentze, M. U. Muckenthaler and N. C. Andrews, *Cell*, 2004, **117**, 285.
17 P. T. Lieu, M. Heiskala, P. A. Peterson and Y. Yang, *Mol. Aspects Med.*, 2001, **22**, 1.
18 I. De Domenico, D. McVey Ward and J. Kaplan, *Nat. Rev. Mol. Cell Biol.*, 2008, **9**, 72.
19 N. T. V. Le and D. R. Richardson, *Biochim. Biophys. Acta*, 2002, **1603**, 31.
20 A. M. Merlot, D. S. Kalinowski and D. R. Richardson, *Antioxid. Redox Signaling*, 2012, **18**, 973.
21 Y. Yu, D. S. Kalinowski, Z. Kovacevic, A. R. Siafakas, P. J. Jansson, C. Stefani, D. B. Lovejoy, P. C. Sharpe, P. V. Bernhardt and D. R. Richardson, *J. Med. Chem.*, 2009, **52**, 5271.
22 M. Kolberg, K. R. Strand, P. Graff and K. Kristoffer Andersson, *Biochim. Biophys. Acta*, 2004, **1699**, 1.
23 C. E. Cooper, G. R. Lynagh, K. P. Hoyes, R. C. Hider, R. Cammack and J. B. Porter, *J. Biol. Chem.*, 1996, **271**, 20291.
24 D. S. Kalinowski, Y. Yu, P. C. Sharpe, M. Islam, Y.-T. Liao, D. B. Lovejoy, N. Kumar, P. V. Bernhardt and D. R. Richardson, *J. Med. Chem.*, 2007, **50**, 3716.
25 D. R. Richardson, D. S. Kalinowski, V. Richardson, P. C. Sharpe, D. B. Lovejoy, M. Islam and P. V. Bernhardt, *J. Med. Chem.*, 2009, **52**, 1459.
26 C. Stefani, G. Punnia-Moorthy, D. B. Lovejoy, P. J. Jansson, D. S. Kalinowski, P. C. Sharpe, P. V. Bernhardt and D. R. Richardson, *J. Med. Chem.*, 2011, **54**, 6936.
27 Y. Yu, Y. S. Rahmanto and D. R. Richardson, *Br. J. Pharmacol.*, 2012, **165**, 148.
28 R. H. U. Borges, E. Paniago and H. Beraldo, *J. Inorg. Biochem.*, 1997, **65**, 267.
29 A. Abras, H. Beraldo, E. O. Fantini, R. H. U. Borges, M. A. Da Rocha and L. Tosi, *Inorg. Chim. Acta*, 1990, **172**, 113.
30 C. Stefani, P. J. Jansson, E. Gutierrez, P. V. Bernhardt, D. R. Richardson and D. S. Kalinowski, *J. Med. Chem.*, 2012, **56**, 357.
31 D. Sriram, P. Yogeeswari, P. Dhakla, P. Senthilkumar, D. Banerjee and T. H. Manjashetty, *Bioorg. Med. Chem.*, 2009, **19**, 1152.
32 P. V. Bernhardt, L. Caldwell, T. B. Chaston, P. Chin and D. R. Richardson, *J. Biol. Inorg. Chem.*, 2003, **8**, 866.
33 M. J. Aguirre, M. Isaacs, F. Armijo, L. Basáez and J. H. Zagal, *Electroanalysis*, 2002, **14**, 356.
34 J. Chambers, B. Eaves, D. Parker, R. Claxton, P. S. Ray and S. J. Slattery, *Inorg. Chim. Acta*, 2006, **359**, 2400.
35 M. Lanznaster, A. Neves, A. J. Bortoluzzi, A. M. C. Assumpção, I. Vencato, S. P. Machado and S. M. Drechsel, *Inorg. Chem.*, 2006, **45**, 1005.
36 T. B. Chaston, R. N. Watts, J. Yuan and D. R. Richardson, *Clin. Cancer Res.*, 2004, **10**, 7365.
37 P. V. Bernhardt, P. C. Sharpe, M. Islam, D. B. Lovejoy, D. S. Kalinowski and D. R. Richardson, *J. Med. Chem.*, 2008, **52**, 407.
38 D. Richardson, E. Tran and P. Ponka, *Blood*, 1995, **86**, 4295.
39 A. Y. Lukmantara, D. S. Kalinowski, N. Kumar and D. R. Richardson, *Bioorg. Med. Chem. Lett.*, 2013, **23**, 967.
40 D. B. Lovejoy and D. R. Richardson, *Blood*, 2002, **100**, 666.
41 T. B. Chaston and D. R. Richardson, *J. Biol. Inorg. Chem.*, 2003, **8**, 427.
42 P. Chandler Guha and H. Prasanna Ray, *J. Am. Chem. Soc.*, 1925, **47**, 385.
43 N. P. Buu-Hoi, N. D. Xuong and N. H. Nam, *J. Chem. Soc.*, 1956, 2160.
44 A. Berger, Skokle and E. E. Borgnes, *US Patent*, 3318772, 1967.
45 P. P. T. Sah and C. T. Peng, *Arch. Pharm.*, 1960, **293**, 501.
46 J. Klarer and R. Behnisch, *Preparation of thiosemicarbazides*, USA, 2657234, 1953.
47 L. Qiu, Z. Shi, Q. Mei and Z. Zhao, *J. Chem. Res.*, 2011, **35**, 456.
48 M. J. Arendse, I. R. Green and K. R. Koch, *Spectrochim. Acta, Part A*, 1997, **53**, 1537.
49 M. Bonnet, J. U. Flanagan, D. A. Chan, E. W. Lai, P. Nguyen, A. J. Giaccia and M. P. Hay, *Bioorg. Med. Chem.*, 2011, **19**, 3347.
50 *Bruker, SADABS*, Bruker AXS Inc., Madison, Wisconsin, USA, 2001.
51 *Bruker, APEX2 and SAINT*, Bruker AXS Inc., Madison, Wisconsin, USA, 2001.
52 G. M. Sheldrick, *Acta. Crystallogr., Sect. A: Fundam. Crystallogr.*, 2008, **64**, 112.
53 C. F. Macrae, I. J. Bruno, J. A. Chisholm, P. R. Edgington, P. McCabe, E. Pidcock, L. Rodriguez-Monge, R. Taylor, J. van de Streek and P. A. Wood, *J. Appl. Crystallogr.*, 2008, **41**, 466.
54 D. R. Richardson and E. Baker, *J. Biol. Chem.*, 1992, **267**, 21384.
55 D. R. Richardson and E. Baker, *Biochim. Biophys. Acta*, 1990, **1053**, 1.
56 D. S. Kalinowski, P. C. Sharpe, P. V. Bernhardt and D. R. Richardson, *J. Med. Chem.*, 2007, **50**, 6212.